Adaptive Control of Dual-Stage Actuator for Hard Disk Drives

Masahito Kobayashi, Shinsuke Nakagawa, and Hidehiko Numasato

Abstract— **The design and implementation of adaptive LS-estimation and fault recovery procedure for PZT-actuated milli-actuator were presented. We confirmed that the adaptive estimation method identified the milli-actuator DC-gain precisely and the fault recovery procedure detected the degradation of milli-actuator gain during track-following data-reading/writing operation.**

Index Terms— **Dual-stage actuator, Adaptive control, Estimation, Fault recovery, Hard disk drive (HDD)**

I. Introduction

THE most significant trend in hard disk drive (HDD) technology is that track density and storage capacity are increasing rapidly while access time is being reduced. This trend has led to the need for improved performance of the head-positioning servo system in order to accurately maintain the selected head position along the center of the track in the track-following mode and to provide rapid movement of the head from one selected track to another selected track in the track-seeking mode. The track pitch of a current HDD is about 0.25 μm and the positioning accuracy is approximately 25 nm. To maintain a high level of performance at more reduced track pitch for future HDDs, the servo system must be able to compensate for track mis-registration (TMR) caused by disk vibration, spindle run-out, the resonance modes of components, and external disturbance sources. This can be accomplished by increasing the servo bandwidth of the track-following servo system.

Dual-stage actuators have been proposed as a possible way of achieving a wider servo bandwidth. A number of control servo designs for the track following mechanism have been discussed in several papers[1], [2], [8]. The track seeking performance of dual-stage servos has also been addressed in some papers[3]. There are three different types of dual-stage actuators; a moving suspension-type milli-actuator, a moving slider-type micro-actuator, and a moving head-type actuator. The voice coil motor (VCM) is used in the first stage to generate large but coarse and slow movement, while the micro/milli-actuator is used in the secondary stage to provide fine and fast positioning. The mechanism for positioning the dual-stage actuator can improve both the track-following and the track-seeking performance.

In the moving suspension type of dual-stage actuator[4] (see **Figure 1**), the milli-actuator is located between the head suspension and the base-plate, which is moved by the VCM actuator. Each head is moved by each milli-actuator and each milli-actuator consists of two push-pull piezoelectric (PZT) elements. Usually, as the milli-actuator does not have a relative distance sensor output and only the head position output is detectable, the total plant of the dual-stage actutor is a double-input single-output (DISO) system. In order to obtain accurate track-following and high-speed track-seeking performance, it is important to identify an accurate value of the PZT gain of each milli-actuator. Moreover, in maintaining performance, it is imprtant to detect degradation of the PZT gain and inform the host system of the possibility actuator fauilure. Since the conventional adaptation method[6], [7] cannot be easily applied to the DISO system, no research has been done about an adaptive control for the milli-actuator of the DISO system.

In the moving slider-type dual-stage actuator, the micro-actuator is located between the suspension and the slider. The advantage of this type is that the collocation of the actuator and sensor head, so a servo bandwidth of 5 kHz or more, is possible. Some micro-actuators has a relative positioning sensor which indicates the micro-actuator movement distance. If the micro actuator has a relative position, the total plant is a double-input double-output (DIDO) system and the adaptation for the micro-actuator can be easily achieved using the relative position[8].

In this paper, we first discuss design and implementation of an adaptive control scheme for a dual-stage actuator without the relative position of the milli actuator. The scheme can be easily applied to the micro-actuator system without relative position. We then propose a fault recovery procedure to detect milli actuator gain degradation during track-following operation. Simulations and experiments show that the proposed adaptive system has good accuracy estimation and an effective on-line adaptation for the dual-stage actuator system in HDD.

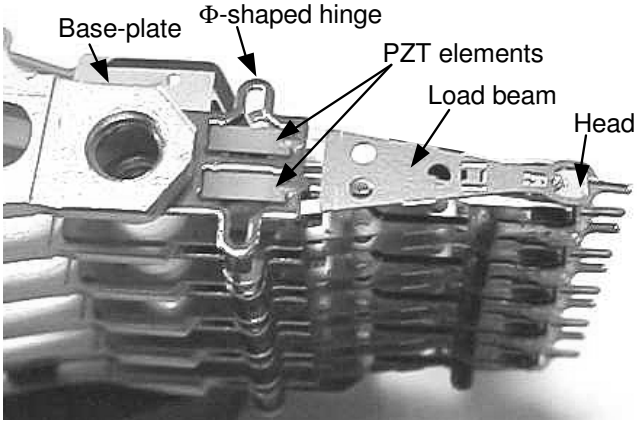

Fig. 1. Moving-suspension type dual-stage actuator

Masahito Kobayashi and Shinsuke Nakagawa are with Storage Technology Research Center, Research & Development Group, Hitachi, Ltd., Japan, kobaya@rd.hitachi.co.jp and naks@rd.hitachi.co.jp

Hidehiko Numasato is with Advanced Technology, Hitachi Global Storage Technologies, Inc., Japan, hidehiko.numasato@hgst.com

0-7803-8335-4/04/$17.00 ©2004 AACC

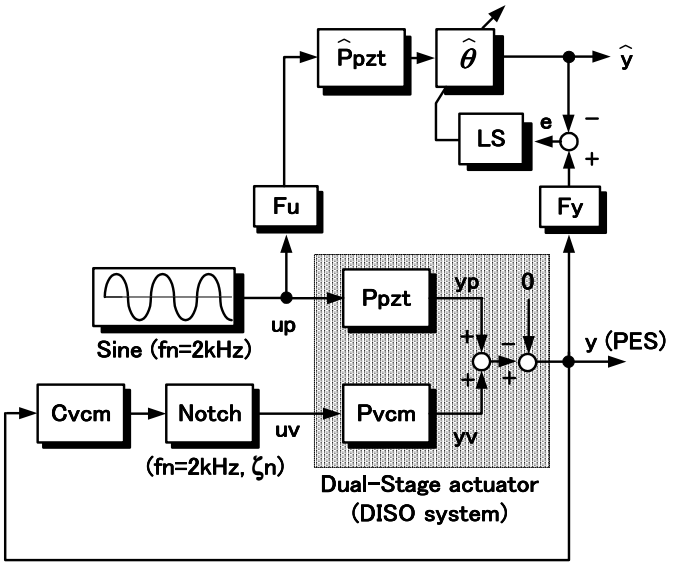

Fig. 2. Block diagram of off-line adaptive LS-estimation

II. Adaptive DC-gain LS-estimation method

In this section, we discuss the design and implementation of an off-line adaptive scheme for estimating the DC-gain of the PZT actuated milli-actuator for a double-input single-output (DISO) system.

A. Moving suspension type dual-stage actuator

Figure 1 shows Φ-shaped dual-stage milli-actuators[4] attached to each carriage arm. The two PZT elements, polarized in opposite directions, are mounted in parallel on a Φ-shaped baseplate hinge with a central beam. The top surfaces of the two PZT elements are electrically connected by a wire and the bottom surfaces of each PZT element are adhesively bonded to the base-plate hinge. When a voltage is applied to both single-ended PZT elements, one PZT element extends, and the other one contracts. The push-pull actuation of the PZT elements moves the head in the off-track direction.

The PZT moving-suspension milli-actuator has the following specifications: mass, 75 mg; suspension length, 14.5 mm; stroke, ± 1 μm/± 30 V; shock resistance, 3,000 G at 0.2 ms half sine. The PZT elements have dimensions of $2.8 \times 1.0 \times 0.15$ mm. The milli-actuators were installed in a 3.5-inch prototype HDD at a rotation speed of 10 krpm. The track pitch is 0.75 μm, and the sampling frequency is about 25 kHz.

In general, when the maximum driving voltage ± 30 V is applied to the PZT milli-actuator, the head position changes ± 1 μm. However, the relationship between the driving voltage and the moving distance of the head (input-output DC-gain characteristics of the actuator) varies about more than 10% due to variations in the manufacturing process of the piezoelectric elements, variations of the piezoelectric element with time, and environmental conditions such as temperature and humidity[5].

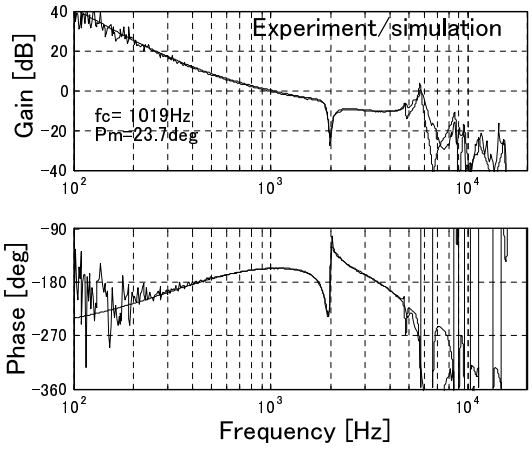

Fig. 3. Frequency response of VCM open loop for off-line adaptation

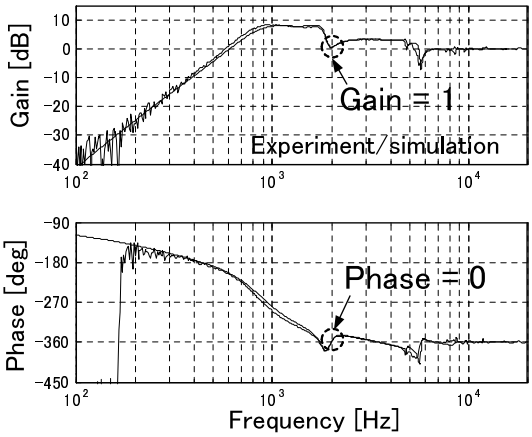

Fig. 4. Frequency response of VCM error rejection for off-line adaptation

B. VCM loop shaping design for DISO system estimation

Figure 2 shows a block diagram of the adaptive LS-estimation system for the milli-actuator with the track following servo system of the VCM actuator.

The dual-stage actuator is operated by two control inputs: a first input u_v to the coarse-movement VCM actuator and a second input u_p to the fine-movement PZT actuator. A head positioning signal y indicating the total movement of the head, obtained by adding the movement of the VCM actuator y_v to that of the PZT actuator y_p, is outputted as an output signal. As a matter of fact, the deviation of the head movement from position information which has previously been recorded on the disk is detected as the Position Error Signal (PES). Thus, the dual-stage actuator is a double-input and single-output (DISO) system and it is difficult to implement a conventional adaptive estimation method[6], [7] of a single-input single-output (SISO) VCM actuator in the DISO system.

As for the VCM actuator, its input-output characteristics can be estimated easily using conventional identification methods, by interrupting the driving voltage to the PZT actuator and letting the VCM actuator operate alone. On the other hand, for the estimation of the input-output

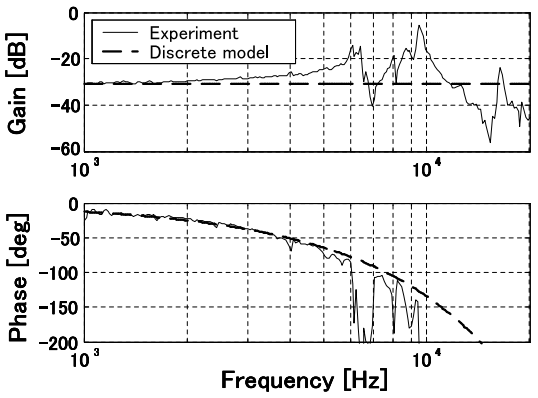

Fig. 5. Frequency response of exprimental PZT milli-actuator and simulated plant model for estimation

characteristics of the PZT actuator, it is difficult to let the PZT actuator operate alone in the positioning without the VCM actuator operation, since the stroke of the milli-actuator is too small relative to various external disturbances to the actuator. Therefore, only the PES (total movement of the VCM and PZT actuator) can be used for the adaptive estimation.

The adaptive LS (least-squares) estimation system in Figure 2 identifies the mill-actuator gain precisely using the PES (y) and the PZT input signal u_p with excitation of sine input ($\pm g_0 \sin(2\pi f_n \cdot k)$), while the head does not read/write the data. The transfer function from the PZT input u_p to the head position y is described as,

$$y = \frac{1}{1 + P_{vcm}C_{vcm}} P_{pzt} \cdot u_p. \tag{1}$$

In order to reject the interference of the VCM servo loop characteristic during the estimation, the notch filter is set in the VCM loop to shape the VCM error rejection $1/(1 + P_{vcm}C_{vcm})$ (from y_p to y) into gain 1 (0 dB) at a specific sine-wave frequency f_n for PZT actuator.

From the viewpoint of the stability and time transient response of the VCM loop, the crossover frequency of the open loop is set to 1 kHz, the cutoff frequency of the notch filter is set to 2 kHz and the damping ratio of the notch filter is set to 0.1. **Figure 3** shows both simulation and experiment of the VCM open loop characteristics. The crossover frequency is 1 kHz and the phase margin is 24 degrees. **Figure 4** shows the error rejection characteristics of the VCM loop. The figures indicate that the gain of the VCM error rejection is 1 (0 db) and the phase is 0 degrees at a frequency of 2 kHz which is the same frequency as the PZT actuated frequency f_n during the estimation period. Thus, the relationship between u_p and y (eq. (1)) can be expressed by the simple equation, where

$$y = P_{pzt} \cdot u_p \qquad \text{at } f_n \text{ (2 kHz frequency)} \tag{2}$$

and we can use the conventional LS-estimation method for the above equation as described below.

C. Adaptive LS-estimation design

The recursive LS-estimation method shown in Figure 2 is explained in detail in the following. In order to reject the noise components from the signals u_p and y, the band-pass filter F_u, F_y which cut-off frequency is 2kHz is used for each signal. For the sake of simplicity, the input u_p and output y will also be used after filtering by the same reference expression. A discrete time model of the milli-actuator from input u_p to the output y_p is expressed by the following equation, in which mechanical resonance is ignored. The calculation time delay is modeled by using first-order Pade approximation and the PZT driver characteristics is modeled by using first-order low-pass filter.

$$y_p(k) = \theta \frac{b_1 \cdot z^{-1} + b_0 \cdot z^{-2}}{1 + a_1 \cdot z^{-1} + a_0 \cdot z^{-2}} u_p(k) \tag{3}$$

where z^{-1} denotes the unit delay operator. The unknown loop gain θ of the plant is composed of the gain of the D/A converter, the gain of the PZT driver, the sensing gain of the head position and the gain of the PZT milli-actuator. **Figure 5** shows the experimental milli-actuator dynamics and simulated plant model described by equation (3). In the figure, since the increase value of the milli-actuator gain dynamics at 2 kHz is small, the milli-actuator resonance characteristic can be neglected.

The above equation can be represented as a regression form,

$$\begin{aligned} y_p(k) &= \theta(b_1 u(k-1) + b_0 u(k-2)) \\ &\quad + (-a_1 y_p(k-1) - a_0 y_p(k-2)) \\ &= \theta \cdot \zeta(k) + \eta(k). \end{aligned} \tag{4}$$

The goal is to estimate a variable gain $\hat{\theta}(k)$ as a good estimation of the loop gain θ from $y_p(k)$, $\zeta(k)$ and $\eta(k)$. Here, the estimation of θ is carried out by use of the recursive least-squares (LS) method. Incidentally, $y_p(k)$ and the head position error $y(k)$ become equal to each other after a certain length of time. Therefore, θ can be estimated by using an observable signal $y(k)$ assuming $y_p(k) = y(k)$ in the above expression.

For the estimation expression (3), an estimator model and estimation error are described as,

$$\hat{y}(k) = \hat{\theta}(k-1) \cdot \zeta(k) + \eta(k), \tag{5}$$

$$e(k) = y(k) - \hat{y}(k). \tag{6}$$

The recursive adaptive adjustment rule updates the gain estimation value $\hat{\theta}(k)$ using the following algorithm[6], [9],

$$\hat{\theta}(k) = \hat{\theta}(k-1) + \frac{\gamma(k-1) \cdot \zeta(k)}{1 + \gamma(k-1) \cdot \zeta(k)^2} e(k) \tag{7}$$

$$\gamma(k) = \frac{\gamma(k-1)}{1 + \gamma(k-1) \cdot \zeta(k)^2} \tag{8}$$

where the initial estimation value is $\hat{\theta}(0) = 0$ and the initial learning gain is set to $\gamma(0) > 0$.

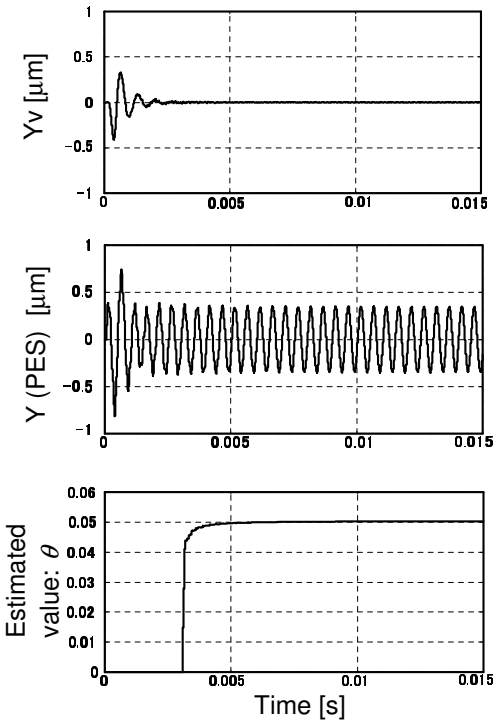

Fig. 6. Simulated time response of off-line LS-estimation (VCM position y_v, PES y and estimated value $\hat{\theta}$)

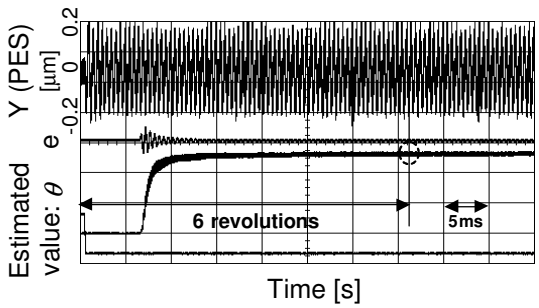

Fig. 7. Exprimental exposed time response of off-line LS-estimation (PES y, estimated error e and estimated value $\hat{\theta}$)

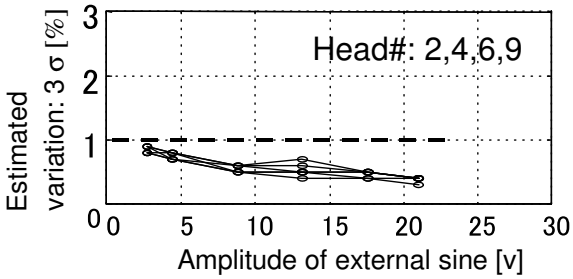

Fig. 8. Estimation accuracy at each head under different input sine voltages

D. Simulation and experimental results

Figure 6 shows the simulated time response waveforms during LS-estimation period. The upper and middle figures show the positions of the output VCM response y_v and the position error signal y, respectively, when a sine wave voltage ($\pm$10 V amplitude, 2 kHz frequency) is applied to the milli-actuator. The VCM position y_v responds with a sine wave-like signal until 0.003 sec due to transient of the notch filter and then converges to zero. This means that observed y perfectly coincides with milli-actuator response y_p from 0.003 sec forward. The bottom figure shows the estimated gain value $\hat{\theta}$ by the LS-estimation which was started at 0.003 sec. The estimated value converged on a correct value in a short time with high accuracy.

The developed off-line LS-estimation method was implemented on a 3.5-inch prototype HDD (10k rpm disk rotation speed) with a moving suspension-type Φ-shaped milli-actuator (see Fig. 1). **Figure 7** shows the 300 exposed time responses during the estimation period (6 disk revolutions: 36 ms). The head position y moves $\pm$ 0.2 μm when the sine wave voltage ($\pm$6 V amplitude, 2 kHz frequency) is applied to the milli-actuator. The estimated value converged on a correct value in 10 ms. We measured estimation value 1000 times on each different head at different input voltages from 3 V to 22 V. The estimated variation with 3σ deviation is within 1.0% value of its actual value as shown in **Figure 8**.

III. Real-time gain estimation and fault recovery procedure

The goal of the second design is to enable an online adaptive estimation method which estimates the input-output characteristics of the PZT milli-actuator and detects its gain degradation even in the midst of data reading/writing. When degradation of the milli-actuator gain is detected, the off-line adaptive gain estimation described in chapter 2 will be executed to obtain a precise value of the mill-actuator gain again and set the appropriate value into PZT controller. Thus, the system can keep its servo performance and reliability in the HDD.

A. Adaptive real-time estimation design

An adaptive real-time estimation method for milli-actuator DC-gain degradation is presented. In this scheme, a gain estimator identifies the loop gain of the milli-actuator during the R/W track following phase, and determines the amount of degradation for each PZT gain. **Figure 9** shows the block diagram of the real-time PZT gain estimation method without injection of any external signal. The dual-stage actuator (DISO system) is stabilized by the decoupled-type controller[2] in this application. The output of a milli-actuator model M_{pzt} is added into an additional reference signal for the VCM actuator, which prevents the PZT actuator from going to the end of its stroke limit and maintains the PZT output on the center of the track. The crossover frequency of the milli-actuator is set at 2.3 kHz.

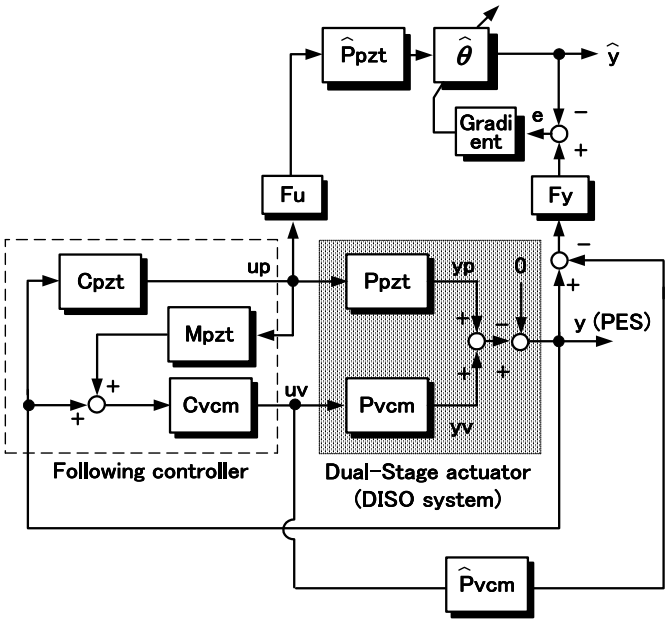

Fig. 9. Block diagram of real-time adaptive gradient-estimation

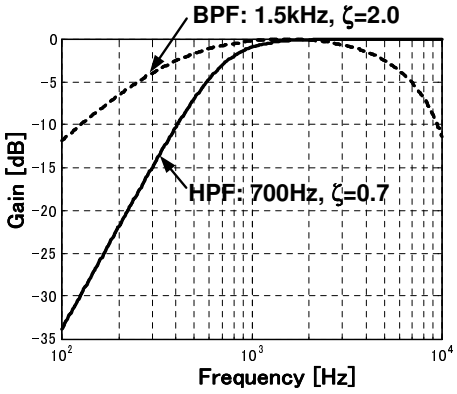

Fig. 10. Frequency response of noise rejection filters (F_u and F_y) for real-time adaptation

In the figure, the estimated output signal of PZT milli-actuator P_{pzt} is calculated by subtracting the output signal of the VCM actuator model $\hat{P}_{vcm}$ from the head position signal y. The VCM model described in the discrete time expression is composed of a second-order low-pass filter. For real-time calculation, the calculation load should be minimized. The adaptive gradient method[9] which cost function J with equation (6) is defined as below, is used for gain estimation.

$$J(k) = e^2(k) \tag{9}$$

By using partial differentiation of the above cost function, the gradient estimate equation with the variable gain $\hat{\theta}(k)$ is obtained as follows,

$$\begin{aligned} \hat{\theta}(k) &= \hat{\theta}(k-1) - \sigma \frac{\partial J(k)}{\partial \hat{\theta}(k)} \\ &= \hat{\theta}(k-1) + 2\sigma \cdot \zeta(k) \cdot e(k) \end{aligned} \tag{10}$$

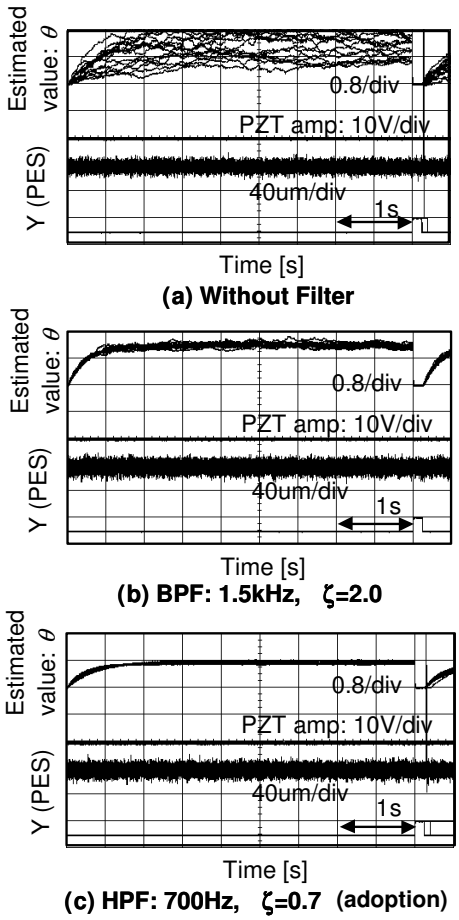

Fig. 11. Exprimental exposed time response of real-time gradient-estimation with each noise rejection filter at different disk location (estimated value $\hat{\theta}$ and PES y)

where σ denotes the learning gain. The amount of calculation by the above equation is extremely smaller in comparison with the equation (7) and (8). On the other hand, estimation accuracy and/or estimation speed might deteriorate slightly.

B. Simulation and experimental results

The three designs of noise rejecting filter F_u and F_y in Figure 9 are evaluated in terms of estimation value and estimation variance. In order to reject the disturbances contaminating the head position signal y and the modeling error of $\hat{P}_{vcm}$ and $\hat{P}_{pzt}$, the second-order band-pass filter at 1.5 kHz ($\zeta = 2.0$), the second-order high-pass filter at 700 Hz ($\zeta = 0.7$) and without filter (gain=1) are designed as shown in **Figure 10**. The estimation was carried out at three different locations (inner/middle/outer disk). **Figure 11** shows the time responses of the estimation value $\hat{\theta}$ and position signal y during estimation for evaluating each noise rejection filter. In the case where there was no filter and there was a band-pass filter, the each estimation variation is large depending on the head location. Using the second-order high-pass filter which rejects more low frequency

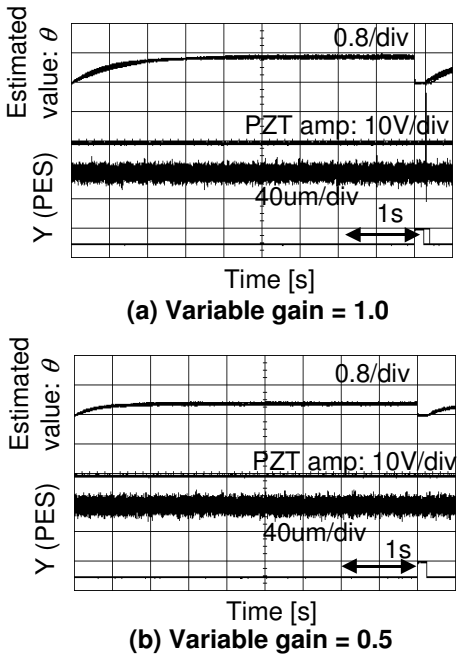

Fig. 12. Exprimental time response of real-time gradient-estimation under DC-gain change from nominal to half value

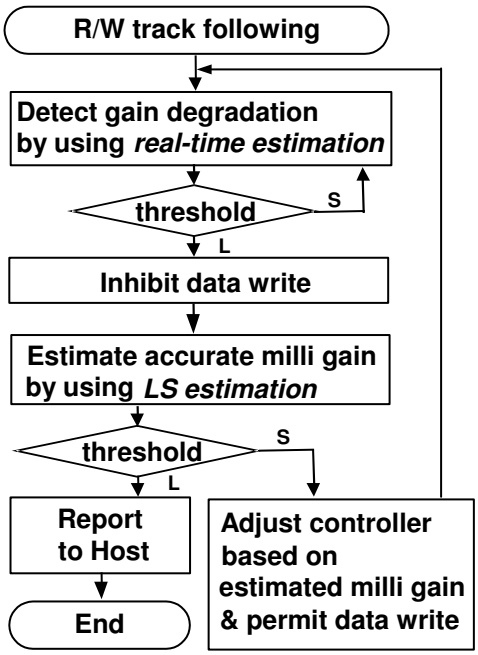

Fig. 13. Fault recovery flow chart for dual-stage actuator gain degradation

VCM input compornents for force disturbances, a small estimation variation (less than 5% in 3σ) is achieved and the filter is adopted for evaluation. The estimation time is about 1.5 sec. The convergence speed is slower than that in the off-line LS-estimation. However, no particular problem arises when the degradation of the milli-actuator with time is estimated. In **Figure 12**, the accuracy of estimation can be seen when the gain of the milli-actuator was intentionally changed from 1.0 to 0.5. The gradient estimator identified the gain change correctly during the track following mode.

C. Fault recovery for milli-actuator gain degradation

Figure 13 is a flow chart showing a fault recovery process is carried out when the milli-actuator gain drop is detected by the real-time estimation (equation (10)). When a estimated gain drop below a preset threshold value is detected, data reading/writing by the head is prohibited and thereafter the gain of the milli-actuator is estimated correctly according to the off-line LS-estimation method (equations (7)(8)). Subsequently, the estimate value obtained by the LS-estimation is compared with the threshold value. If the difference between the estimated value and the threshold value is small, the milli-actuator controller C_{pzt} is adjusted based on the estimation result. Thereafter, a flag permitting the data read/write is turned on and the dual-stage actuator track following returns to its normal state. On the other hand, if the difference between the estimated value and the threshold value is large, an alarm is issued to the upper level holst controller. In such cases of gain drop below the threshold value, the data reading/writing might become impossible, and there is a possibility of failure of the milli-actuator caused by some factors.

IV. Conclusions

The design and implementation of adaptive estimation method and a fault recovery scheme for a PZT-actuated milli-actuator were presented. We confirmed that the off-line adaptive LS-estimation method identified the milli-actuator DC-gain precisely within 1.0% value (3σ) of its actual value in 36 ms. We also confirmed that the fault recovery method detected the degradation of milli-actuator gain within 5.0% value in 1.5 sec and collected the gain properly.

References

[1] T. Semba, T. Hirano, J. Hong and L.S. Fan, "Dual-stage servo controller for HDD using MEMS microactuator,"*IEEE Trans. on Magnetics*, vol.35, no.5, pp.2271-2273, 1999.

[2] M. Kobayashi, S. Nakagawa and S. Nakamura, "A phase-stabilized servo controller for dual-stage actuators in hard disk drives,"*IEEE Trans. on Magnetics*, vol.39, no.2, pp.844-850, 2003

[3] M. Kobayashi and R. Horowitz, "Track seek control for hard disk dual-stage servo systems,"*IEEE Trans. on Magnetics*, vol.37, no.2, pp.949-954, 2001

[4] M. Tokuyama, T. Shimizu, H. Masuda, S. Nakamura, M. Hanya, O. Iriuchijima and J. Soga, "Development of a Φ-shaped actuated suspension for 100-kTPI hard disk drives,"*IEEE Trans. on Magnetics*, vol.37, no.4, pp.1884-1886, 2001

[5] S. Nakamura, I. Naniwa, K. Sato, K. Yasuna and S. Saegusa, "Life-time prediction method for piggyback PZT actuator,"*IEEE Trans. on Magnetics*, vol.37, no.2, pp.940-943, 2001

[6] M. Kobayashi, T. Yamaguchi, H. Hirai, K. Tsuneta, T. Arai and K. Onoyama, "Adaptive control of a hybrid servo system for magnetic disk drives,"*JSME International Journal*, series C, vol. 39, no. 4, pp.772-780, 1996

[7] R. Horowitz and B. Li, "Adaptive track-following servos for disk file actuators,"*IEEE Trans. on Magnetics*, vol.32, no.3, pp.1779-1786, 1996

[8] Y. Li and R. Horowitz, "Mechatronics of electrostatic microactuators for computer disk drive dual-stage servo systems,"*IEEE/ASME Trans. on Mechatronics*, vol.6, no.2, pp.111-121, 2001

[9] G.C. Goodwin and K.S. Sin, "Adaptive filtering prediction and control,"*Prentice Hall*, 1984